Inhibition of T7 RNA Polymerase: Transcription Initiation and Transition from Initiation to Elongation Are Inhibited by T7 Lysozyme *via* a Ternary Complex with RNA Polymerase and Promoter DNA†

Amarendra Kumar and Smita S. Patel*

Department of Biochemistry, The Ohio State University, 484 West 12th Avenue, Columbus, Ohio 43210

Received June 16, 1997; Revised Manuscript Received September 2, 1997⊗

ABSTRACT: The mechanism of transcription repression of T7 RNA polymerase by T7 lysozyme was investigated using a combination of kinetic and equilibrium methods. HPLC gel-filtration experiments demonstrated complex formation between T7 lysozyme, T7 RNA polymerase, and promoter DNA. The interactions between the two proteins were quantitated by measuring in real time the changes in protein fluorescence upon binary complex formation using stopped-flow kinetics. Complex formation between T7 lysozyme and the RNA polymerase was found to occur by a one-step process, with a bimolecular association rate constant of 38 μM^{-1} s^{-1} and a dissociation rate constant of 3.5 s^{-1}. These constants provided an equilibrium dissociation constant, K_d, of 92 nM for the polymerase·lysozyme complex. The interactions of the polymerase with the DNA were studied by stopped-flow kinetics and nitrocellulose equilibrium DNA binding experiments in the absence and in the presence of T7 lysozyme. The results showed that T7 lysozyme did not prevent or change the kinetic or thermodynamic interactions of the RNA polymerase with the DNA. T7 lysozyme by itself did not bind to the DNA, but since it bound to the RNA polymerase as well as to the polymerase·DNA complex, transcription repression must involve the formation of the ternary complex between T7 lysozyme, T7 RNA polymerase and the promoter DNA. The effect of T7 lysozyme was most striking on runoff product synthesis which was greatly inhibited whereas the steady-state synthesis of abortive products, limited by polymerase cycling or RNA dissociation, was relatively unaffected by the presence of T7 lysozyme. Investigation of the pre-steady-state kinetics of transcription in the presence and absence of T7 lysozyme indicated that the inhibition of runoff product synthesis was largely due to inhibition of transcription initiation and transition from initiation to elongation.

Transcription by T7 RNA polymerase[1] is regulated both by the gradual entry of the phage DNA into the host *Escherichia coli* cell (McAllister et al., 1981) and by T7 lysozyme protein (Moffatt & Studier, 1987), a product of T7 gene 3.5. T7 lysozyme is a 17 kDa protein that has two distinct functions: It cuts a peptide bond in the peptidoglycan layer of the host cell wall to assist cell lysis, and it also inhibits transcription by T7 RNA polymerase. It plays a role in both shutting down transcription of late T7 genes and in initiating of T7 DNA replication (Studier, 1972; Silberstein et al., 1975; McAllister & Wu, 1978). It has been shown that T7 lysozyme forms a specific complex with T7 RNA polymerase (Moffatt & Studier, 1987), but the interactions have not been quantitated. The X-ray structures of T7 RNA polymerase (Sousa et al., 1993) and T7 lysozyme (Cheng et al., 1994) are known, but the X-ray structure of T7 lysozyme·T7 RNA polymerase complex has not yet been determined. Detailed genetic studies, however, have identified amino acids and regions of the two proteins that may be involved in protein−protein interactions (Moffatt & Studier, 1987; Cheng et al., 1994).

The mechanism by which T7 lysozyme inhibits transcription is not understood at the kinetic or the thermodynamic level. Here we have investigated the mechanism of repression by investigating if T7 lysozyme inhibited transcription by a competition mechanism whereby T7 lysozyme would compete with the RNA polymerase for binding to the promoter DNA. Similarly, experiments were designed to determine which stage of transcription—initiation, transition from initiation to elongation, or elongation—was most affected by T7 lysozyme. The results reported here indicate that T7 lysozyme by itself does not bind to the DNA but it forms with T7 RNA polymerase and promoter DNA a ternary complex which has lower activity. T7 lysozyme inhibits both transcription initiation and transition from initiation to elongation to about the same extent. Many of the similar questions were addressed by Zhang and Studier (1997) in their recent report using different biochemical techniques, and the results from both studies are in agreement. The exact mechanism by which initiation and promoter escape processes are inhibited by T7 lysozyme still remains to be determined. Nevertheless, the present studies lay the foundation for more detailed future investigation of the repression mechanism. More detailed studies will allow one to decipher interesting and perhaps new ways by which transcription can be regulated by protein−protein interactions.

* Corresponding author. Tel: (614) 292-7763. Fax: (614) 292-6773. E-mail: Patel.85@osu.edu.

† This research was supported by NIH Grant GM51966 and by a Junior Faculty Research Award from the American Cancer Society (JFRA 565) to S.S.P.

⊗ Abstract published in *Advance ACS Abstracts,* November 1, 1997.

[1] Abbreviations: E, T7 RNA polymerase; L, T7 Lysozyme; D, Φ10 promoter DNA; pppGpG, guanylyl(3′−5′)guanosine triphosphate; rNTP, ribonucleoside 5′-triphosphate; 2-AP, 2-aminopurine; ds, double stranded.

S0006-2960(97)01432-3 CCC: $14.00

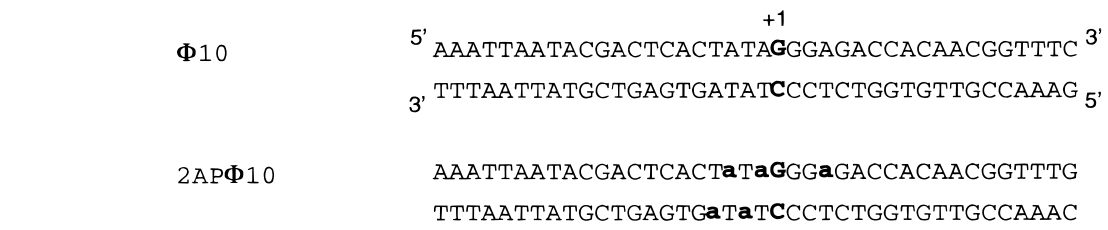

FIGURE 1: Sequences of T7 DNA promoters. The upper and lower rows represent the sequence of the nontemplate and the template strands of the promoter DNA. Transcription initiation site (+1) is marked by bold capital letters. The positions of the modified base 2-aminopurine are shown as "**a**".

EXPERIMENTAL PROCEDURES

Protein Purification

T7 RNA polymerase was purified (Grodberg & Dunn, 1988) from an overexpressing *E. coli* strain BL21/pAR1219 (Davanloo et al., 1984) generously provided by Alan Rosenberg and Bill Studier, Brookhaven National Laboratories. The enzyme was >95% pure after elution through three chromatographic columns consisting of SP-Sephadex, CM-Sephadex, and DEAE-Sephacel purchased from Sigma. The enzyme was stored at −80 °C after dialyzing against the buffer containing 50% glycerol (v/v), 20 mM sodium phosphate, pH 7.7, 1 mM trisodium EDTA, 1 mM dithiothreitol, and 100 mM NaCl. The concentration of the enzyme was determined from its absorbance and molar extinction coefficient of 1.4×10^5 M^{-1} cm^{-1} at 280 nm (King et al., 1986). T7 lysozyme was purified according to a reported procedure (Cheng et al., 1994). We thank Alan Rosenberg and Bill Studier (Brookhaven National Laboratories) for kindly providing the BL21/pAR4593 cell line.

Synthesis of Oligonucleotides: Normal and 2-Aminopurine (2-AP) Modified Analog

All the oligonucleotides used in this study (Figure 1) were synthesized on a Millipore Nucleic Acid synthesis system 899. DMT−deoxynucleoside (benzoyl or isobutyryl) β-cyanoethylphosphoramidites were purchased from PerSeptive Biosystems. The 2-aminopurine CE and Ac-dC-CE phosphoramidites were purchased from Glen Research Corp. The synthesis, purification, and determination of concentration of these promoter DNAs were according to the procedures described in our previous study (Jia et al., 1996). The double-stranded (ds) DNAs were prepared by annealing the individual single-stranded (ss) DNA strands. The exact ratio of the two ss DNA strands used to prepare the ds DNAs was determined from titration experiments performed on a 18% native polyacrylamide gel that resolves ds DNA from the ss DNAs.

HPLC Gel-Filtration

Complex formation between T7 lysozyme and T7 RNA polymerase was investigated by gel-filtration chromatography. The chromatography was carried out on an HPLC instrument (Waters 625 LC 625) using a size-exclusion column (Bio-Rad, molecular weight range, 20 000−1 000 000, pore size, 400 Å), and the proteins were detected using a Waters 470 (Millipore) fluorescence detector ($\lambda_{excitation} = 290$ nm and $\lambda_{emission} = 345$ nm). Chromatography was performed at room temperature using an elution buffer that contained 50 mM Tris acetate (pH 7.5), 100 mM sodium acetate, and 10 mM magnesium acetate.

Rapid Chemical Quench-Flow Experiments and Analysis of the Transcription Products

The pre-steady-state kinetic experiments were carried out on a rapid chemical quench-flow instrument (KinTek Corp., State College, PA). A typical pre-steady-state experiment was carried out as follows. T7 RNA polymerase (30 μM) and 40-mer Φ10 promoter DNA (20 μM) were preincubated in the presence or absence of T7 lysozyme (36 μM) in a buffer containing 50 mM Tris acetate, 100 mM sodium acetate, 10 mM magnesium acetate, and 5 mM DTT and loaded in one syringe. In another syringe was loaded, a buffer (50 mM Tris acetate, 10 mM magnesium acetate, and 5 mM DTT) containing 500 μM of each of the four rNTPs (GTP, ATP, CTP, and UTP; all from Sigma Chemical Co.) spiked with [γ-^{32}P]GTP (from Amersham). A constant temperature of 25 °C was maintained using a water bath. Transcription reaction was initiated by rapidly mixing equal volumes of the two solutions in the quench flow instrument. After 50 ms to 25 s, the reactions were quenched by rapidly mixing with 1 N HCl. Chloroform was then added and the reactions were neutralized with base (0.25 M Tris base and 1 M NaOH).

The RNA products, 2-mer through 19-mer, were resolved by electrophoresis at 55 °C (110 W) on a highly cross-linked 23% polyacrylamide/3 M urea gel on a Bio-Rad sequencing gel apparatus (comb thickness, 0.25 mm). The gel was exposed to a phosphor screen for 12−15 h and scanned on a PhosphorImager instrument (Molecular Dynamics), and the RNA bands were quantitated using the ImageQuaNT software.

Stopped-Flow Kinetics

The kinetics of E·D or E·L complex formation were measured using a stopped-flow instrument (KinTek Corp., State College, PA). A typical stopped-flow experiment was carried out by rapidly mixing equal volumes (40 μL) of T7 RNA polymerase and T7 lysozyme in a buffer containing 50 mM Tris acetate, pH 7.5, 50 mM sodium acetate, 10 mM magnesium acetate, 5 mM dithiothreitol, and by monitoring the change in protein fluorescence. The samples were excited at 290 nm (slit width, 1 mm), and emission at >348 nm was monitored using a cut-on long-pass filter (Oriel Corp., catalog number 51260). In the experiments where fluorescent (2-AP) DNA analog was used, the 2-AP fluorescence emission was measured using a cut-on filter (>360 nm, WG360, Hi-Tech Scientific, serial number 273129), after excitation at 315 nm (3 mm slit width). About 20−30 traces were averaged in experiments where protein fluorescence

changes were monitored whereas it was sufficient to average 5−10 kinetic traces when 2-AP DNA fluorescence was monitored. All the stopped-flow experiments reported in this paper were conducted at 25 °C.

Equilibrium DNA Binding

The equilibrium binding of DNA to T7 RNA polymerase (at 25 °C) was examined using nitrocellulose filter binding assays (Hingorani & Patel, 1993). The DEAE and nitrocellulose membranes (Schleicher & Schuell) were treated for 10 min with 0.5 M NaOH, washed thoroughly with doubly distilled water, and equilibrated in the binding buffer (50 mM Tris acetate, pH 7.5, 50 mM sodium acetate, 10 mM magnesium acetate, 5 mM dithiothreitol) before the experiment. A typical DNA binding titration was performed at constant polymerase concentration and increasing concentration of ds Φ10 DNA with the nontemplate strand ^{32}P radiolabeled at the 5′ end. The polymerase (3 μM) was preincubated with DNA (0−30 μM), and 8 μL of the mixture at each concentration of DNA was filtered through a layer of nitrocellulose and DEAE membranes under vacuum using a water aspirator. The filters were dried, exposed to phosphor screens, and quantitated on a PhosphorImager. The molar amount of polymerase-bound DNA was calculated from the fraction of DNA bound to the nitrocellulose membrane and of free DNA bound to the DEAE membrane.

Data Analysis

The stopped-flow kinetics traces were fit using the KinTek software to the equation

$$F = \sum A_n \exp(-k_{\mathrm{obs},n}t) + C$$

where F is the fluorescence at time t, n is the number of exponential terms, A_n and $k_{\mathrm{obs},n}$ are the amplitude and the observed rate constant of the n^{th} term, respectively, and C is the fluorescence intensity at $t = 0$.

The pre-steady-state kinetic data were computer fit either to the burst equation (shown below) or a linear equation using SigmaPlot (Jandel Scientific) software.

$$\text{Burst equation: } A(1 - \mathrm{e}^{-kt}) + bt + c$$

where A represents the burst amplitude, k the exponential burst rate constant, b the linear steady-state rate constant, and c the y-intercept.

Kinetic Simulations. All kinetic simulations were performed using the PSUSIM program (kindly provided by Kenneth Johnson, Pennsylvania State University, State College, PA) which is based on the KINSIM program (Barshop et al., 1983). A simplified mechanism of transcription (Scheme 1) was chosen, and simulated curves were generated using the PSUSIM program. Estimates of the kinetic rate constants for the chosen mechanism were obtained from exponential fit to the kinetic data (see above). The kinetic rate constants were adjusted manually during the simulation process to obtain the best agreement between the simulated and the experimental data. The process was continued repeatedly until a good visual fit was obtained between the simulated curves and the experimental kinetic data.

RESULTS

T7 RNA Polymerase Forms a Complex with T7 Lysozyme

It has been shown previously by affinity column chromatography (Moffatt & Studier, 1987) that T7 lysozyme forms a complex with T7 RNA polymerase. We have used HPLC gel-filtration experiments to quantitate the interactions between the two proteins and to investigate the effect of promoter DNA on E·L complex formation. The results showed that T7 lysozyme formed a complex with T7 RNA polymerase both in the absence and in the presence of the promoter DNA (Figure 2), but T7 lysozyme by itself did not bind to the DNA (data not shown). Although T7 lysozyme was well resolved from the RNA polymerase (or the E·D complex) on a size exclusion HPLC column (Figure 2A,B), it was difficult to resolve the E·L complex from the free polymerase. We therefore monitored the disappearance of free L to measure the formation of E·L. When 0.3 μM T7 lysozyme was mixed with 0.3 μM T7 RNA polymerase, almost no complex formation was observed (judging from the lack of decrease in the free T7 lysozyme peak) (Figure 2A). However, when the concentrations of E and L were increased to 10 μM, the free lysozyme peak area decreased and the polymerase peak shifted, demonstrating complex formation between the two proteins. The same results were obtained in the presence of 40-mer Φ10 promoter DNA (Figure 2B). Gel-filtration experiments performed at various protein concentrations were used to determine the equilibrium dissociation constant (K_{d}) of 1−2 μM in the absence and in the presence of DNA (Figure 2C). This K_{d} value of E·L complex is, however, much higher than the K_{d} obtained from the stopped-flow experiments (see below). We believe that the K_{d} from the gel-filtration experiment is likely to be in error because the gel-filtration experiment is strictly not an equilibrium method. If the complex is kinetically unstable, then it will tend to dissociate during the filtration process and the observed K_{d} will be higher than the true equilibrium K_{d}.

Kinetics of T7 Lysozyme·RNA Polymerase Complex Formation

We have used stopped-flow kinetics to quantitate more accurately the interactions between T7 lysozyme and T7 RNA polymerase and to investigate the steps involved in E·L formation. Mixing of T7 lysozyme with T7 RNA polymerase resulted in quenching of intrinsic protein fluorescence. A representative time course of the decrease in fluorescence upon mixing T7 lysozyme with T7 RNA polymerase is shown in Figure 3A. We have probed the kinetics and thermodynamics of E·L formation by measuring the kinetics of fluorescence decrease as a function of lysozyme concentration. The association and dissociation rate constants for E·L formation were obtained from the plot of observed rate constant (k_{obs}) of the decrease in protein fluorescence *versus* [L] (Figure 3B). The linear increase in k_{obs} with increasing [L] suggested one-step binding of T7 lysozyme to the polymerase as shown below:

$$\mathrm{E} + \mathrm{L} \underset{k_{\mathrm{off}}}{\overset{k_{\mathrm{on}}}{\rightleftharpoons}} \mathrm{EL}$$

where $k_{\mathrm{obs}} = k_{\mathrm{on}}[\mathrm{L}] + k_{\mathrm{off}}$. The slope of the k_{obs} *vs* [L]

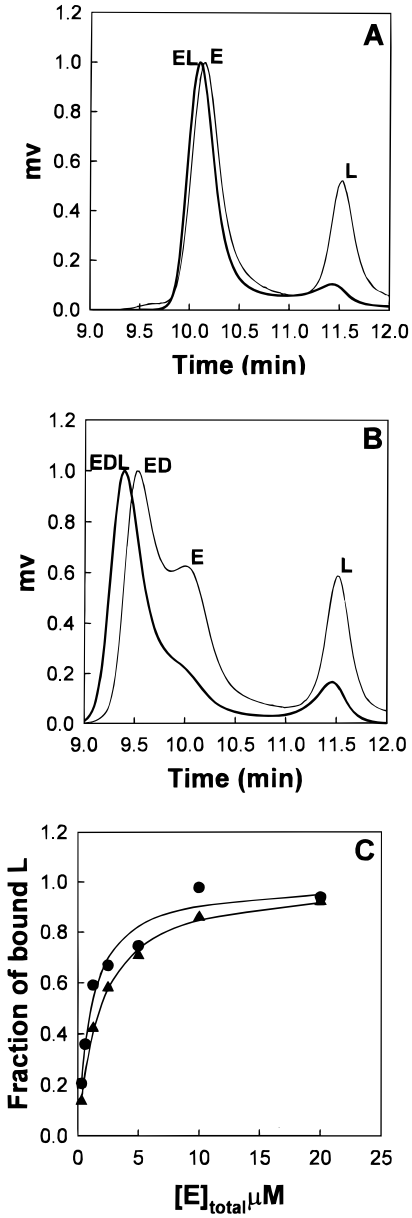

FIGURE 2: HPLC gel-filtration analysis of E·L complex formation in the presence and absence of promoter DNA. A mixture of T7 RNA polymerase and T7 lysozyme was loaded on a HPLC gel-filtration column (see experimental procedures) in the absence (panel A) and in the presence (panel B) of Φ10 promoter DNA. The gel-filtration profiles were normalized, thus the *y*-axis is in arbitrary units. The lighter traces in panels A and B represent data obtained at lower concentration (0.3 μM each) of E, L, and D, while the darker traces represent data at high concentration (10 μM each) of E, L, and D. Panel C is a plot of fraction of bound lysozyme *vs* $[E]_{total}$. Data in the absence of DNA is represented by circles and in the presence of DNA by triangles. Hyperbolic fits of the data gave K_d of 1.1 and 1.8 μM for the E·L and E·D·L complexes, respectively.

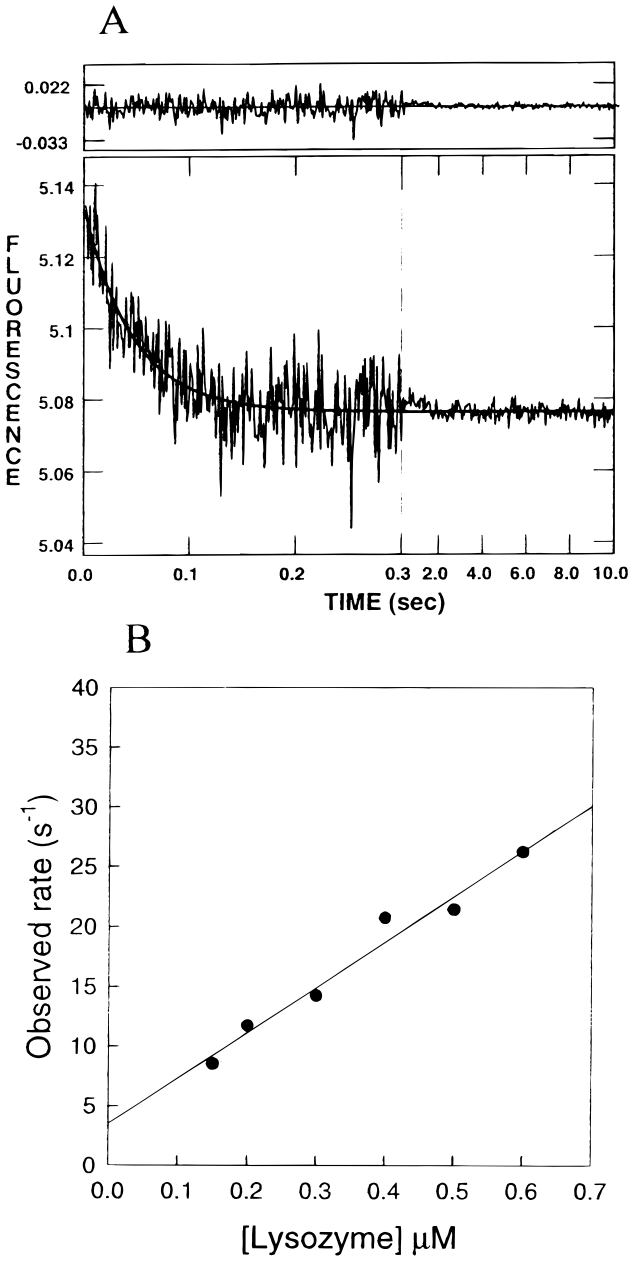

FIGURE 3: Stopped-flow kinetics of E·L complex formation. (A) The kinetic trace (an average of 38 measurements) shows the time-dependent decrease in intrinsic protein fluorescence (excitation at 290 nm and emission >348 nm) after mixing 0.5 μM L and 0.1 μM E (final concentrations). The solid line represents the nonlinear least-squares fit to a single exponential decay with rate constant of 21.43 ± 1.17 s^{-1}. Regression analysis of the curve fitting is shown in the small panel above the kinetic trace. (B) The stopped-flow kinetics of E·L formation was measured at increasing T7 lysozyme concentration. The observed exponential rate constant increased linearly with increasing [L]. The slope provided a k_{on} value of 38 μM^{-1} s^{-1} and the *y*-intercept the k_{off} of 3.5 s^{-1}, and thus a K_d (k_{off}/k_{on}) of 92 nM for the E·L complex.

provided the bimolecular rate constant, k_{on} (38 μM^{-1} s^{-1}), and the intercept provided the dissociation rate constant k_{off} (3.5 s^{-1}) (Johnson, 1992). The ratio k_{off}/k_{on} gave a K_d of 92 nM for the E·L complex.

Effect of T7 Lysozyme on the Steady-State Kinetics of Transcription

To understand the mechanism of transcription repression by T7 lysozyme, it is necessary to determine which stage of transcription is inhibited by T7 lysozyme. For instance, does T7 lysozyme inhibit transcription initiation, the transition from initiation to elongation, or transcription elongation? To answer this question, we first compared the steady-state kinetics of RNA synthesis in the absence and presence of T7 lysozyme. The transcription reactions were carried out using the 40 bp promoter DNA that has natural T7 sequence from −21 to +19 near the F10 promoter region (Figure 1). The experiments were carried out at 25 °C using 2 μM polymerase and 1 μM DNA, and the lysozyme concentration

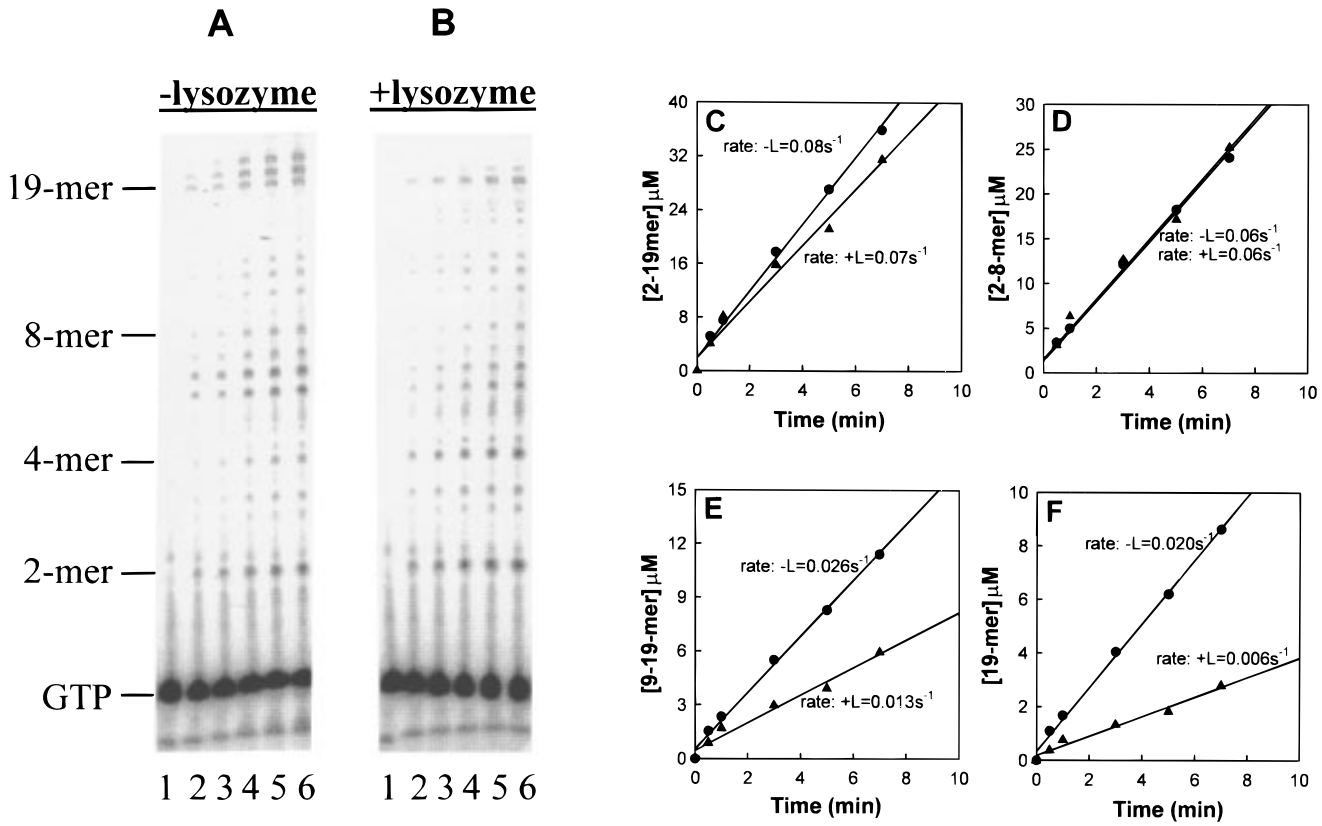

FIGURE 4: Steady-state kinetic analysis of transcription in the absence and presence of T7 lysozyme. T7 RNA polymerase (2 μM) and 40-mer Φ10 promoter DNA (1 μM) in the presence or absence of T7 lysozyme (10 μM) were mixed with all four rNTPs (GTP, ATP, UTP, and CTP, 500 μM each) + [γ-^{32}P]GTP to initiate the reaction. The reactions were acid-quenched and the RNA products were resolved on a 23% polyacrylamide gel (3 M urea). Panels A and B show the PhosphorImager scan of the transcriptional products in the absence and presence of T7 lysozyme respectively. Lanes 1−6 show the products formed in the reactions quenched after 0, 0.5, 1, 3, 5, and 7 min, respectively. Panels C−F depict the steady-state kinetics of total RNA synthesis (2−19-mer), the initiation products (2−8-mer), the elongation products (9−19-mer) and the runoff product (19-mer) respectively, in the absence (●) and in the presence (▲) of T7 lysozyme. The steady-state rates shown were obtained by dividing the linear slopes by concentration of E·D (1 μM).

(10 μM) was well above the K_d of E·L complex. Both abortive and elongation RNA products were monitored by conducting the reactions in the presence of all four NTPs and analyzing the products on a high percentage polyacrylamide gel. Figures 4A and B show the PhosphorImager scan of the RNA products, and Figures 4C−F show the quantitated kinetics in the absence and presence of T7 lysozyme. The kinetics of total RNA (2−19-mer), abortive RNA (2−8-mer), elongation products (9−19-mer) and the runoff product (19-mer) were analyzed separately to determine which stage of transcription was affected by T7 lysozyme.

Within the time scale of the experiment (7 min), the steady-state rate of total RNA synthesis (2−19-mer) in the absence of T7 lysozyme (0.08 s^{-1}) was close to the rate in the presence of T7 lysozyme (0.07 s^{-1}) (Figure 4C). Similarly, no inhibition in the steady-state rate of abortive RNA synthesis (2−8-mer) was observed in the presence of T7 lysozyme (Figure 4D). Only the steady-state rates of elongation (9−19-mer) and runoff product (19-mer) formation were inhibited by 2−3-fold in the presence of T7 lysozyme (Figure 4E,F). Because the steady-state rate of abortive RNA product synthesis is limited by RNA dissociation or polymerase cycling (Jia & Patel, 1997), the above results indicate that T7 lysozyme does not affect those steps. To investigate the effect of T7 lysozyme on transcription initiation, we have measured the pre-steady-state kinetics of RNA synthesis.

Effect of T7 Lysozyme on the Pre-Steady-State Kinetics of Transcription

The pre-steady-state kinetics of RNA synthesis were measured by preincubating RNA polymerase (30 μM) with the promoter DNA (20 μM) and T7 lysozyme (36 μM) and initiating the reactions by adding all four rNTPs + [γ-^{32}P]-GTP. High concentrations of polymerase and DNA were used to accurately measure the kinetics of RNA synthesis in the first turnover of catalysis. The concentration of T7 lysozyme was kept above that of the polymerase to allow 100% complex formation. The kinetics of RNA synthesis under these conditions were measured using a rapid chemical quench-flow instrument. Figures 5A and 5B show the PhosphorImager scan of the RNA products formed under pre-steady-state conditions in the absence and in the presence of T7 lysozyme, respectively. Figures 5C−F show the kinetics of RNA products formed at different stages of transcription reaction.

In the absence of T7 lysozyme, RNA synthesis showed burst kinetics. That is, there was an initial fast exponential phase of RNA synthesis followed by a slower linear phase (Figure 5C). These kinetics indicate that RNA synthesis in the first turnover is faster than synthesis in subsequent turnovers. The rate of transcription initiation can be obtained from the initial linear or the exponential burst rate constant, and the steady-state rate constant is a composite rate constant that measures the rate of polymerase recycling after abortive

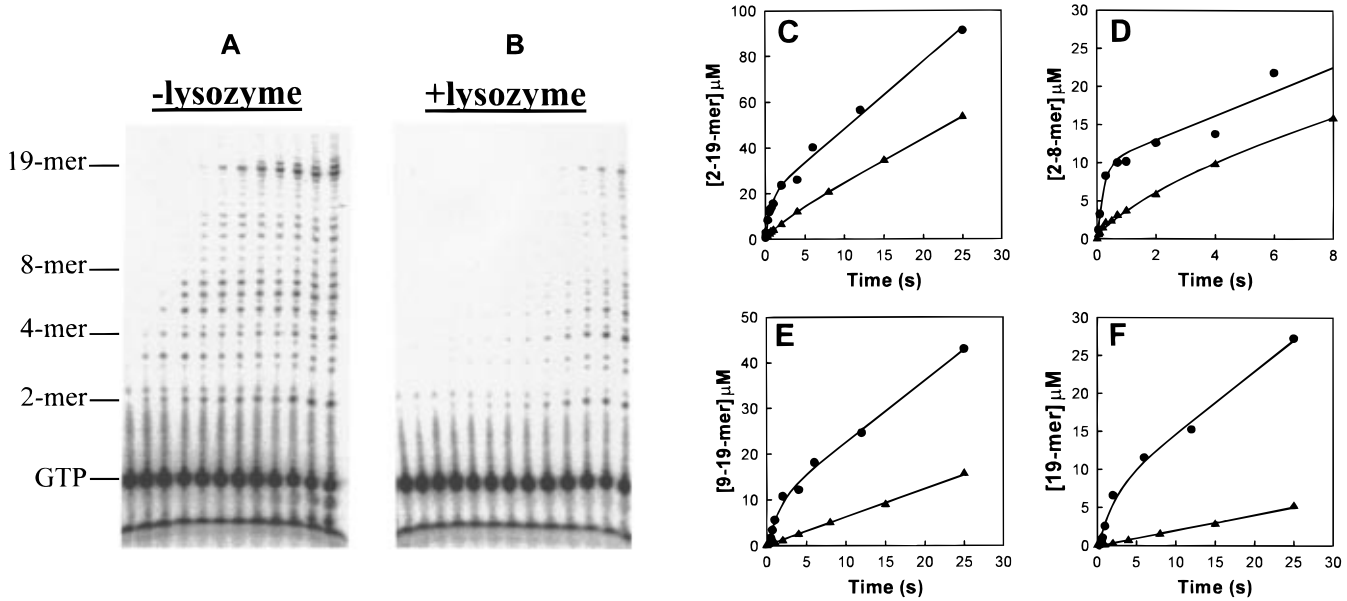

FIGURE 5: Pre-steady-state kinetics of transcription in the absence and presence of T7 lysozyme. T7 RNA polymerase (30 μM) and 40-mer Φ10 promoter DNA (20 μM) in the presence or absence of T7 lysozyme (36 μM) were mixed with all four rNTPs (GTP, ATP, UTP, and CTP, 500 μM each) + [γ-^{32}P]GTP to initiate the reaction. Panels A and B show the phosphorimager scan of the pre-steady-state transcriptional products formed in the absence and presence of T7 lysozyme, respectively. Lanes from left to right in panel A correspond to the reactions quenched after 0, 0.05, 0.1, 0.3, 0.5, 0.7, 1, 2, 4, 6, 12, and 25 s, and lanes from left to right in panel B correspond to reactions quenched after 0, 0.05, 0.1, 0.2, 0.3, 0.5, 0.7, 1, 2, 4, 8, 15, and 25 s. Panels C−F depict the kinetics of various RNA products in the absence (●) and in the presence (▲) of T7 lysozyme. All solid lines, except those for the 9−19-mer and 19-mer in the presence of T7 lysozyme, were fit to the burst equation (see Experimental Procedures). The initial rate constants of RNA synthesis were as follows, in the absence and presence of T7 lysozyme, respectively: 1.26 and 0.15 s^{-1} (2−19-mer); 0.2 and 0.06 s^{-1} (2-mer); 0.9 and 0.36 s^{-1} (2−8-mer); 0.3 and 0.03 s^{-1} (9−19-mer); 0.18 and 0.01 s^{-1} (19-mer).

and elongation product synthesis (Jia & Patel, 1997). T7 lysozyme inhibited the pre-steady-state rate of RNA synthesis but had little effect on the steady-state rate. Thus in the presence of T7 lysozyme the fast burst phase was very small, and the pre-steady-state kinetics were nearly linear (Figure 5C). These results indicate that transcription initiation is inhibited by T7 lysozyme, and the rate of initiation is reduced to an extent that it is either slower or closer to the rate of RNA dissociation or polymerase cycling.

To quantitate the effect of T7 lysozyme on the different stages of transcription, we have compared the initial rate constants of total (2−19-mer), abortive (2−8-mer), elongation (9−19-mer), and runoff (19-mer) product synthesis (Figure 5). Comparison of the initial rate constants showed that total RNA synthesis was inhibited more than 8-fold by T7 lysozyme (Figure 5C), the 2-mer synthesis was inhibited about 3-fold, abortive RNA product about 3-fold (Figure 5D), the elongation products about 9-fold (Figure 5E), and the 19-mer runoff product about 20-fold (Figure 5F) by T7 lysozyme. The processivity of RNA synthesis in the elongation phase (9-mer to 19-mer formation also seemed to be affected by T7 lysozyme, as more intermediate RNA products were found to accumulate in the reaction.

The above pre-steady-state kinetics in the presence of T7 lysozyme were also measured in two more ways. In one experiment, the polymerase was preincubated with the DNA and T7 lysozyme was added with the rNTPs at the start of the reaction. In a second experiment, T7 lysozyme was preincubated with the polymerase and DNA was added along with the rNTPs at the start of the reaction. The polymerase was inhibited to the same extent in all of the above experiments (data not shown). These results suggest that the order of addition of E, D, or L is not important and that E·L or E·D·L complex formation steps are fast and do not limit the inhibition process.

Kinetic Simulation of Transcription in the Absence and Presence of Lysozyme

The pre-steady-state kinetics of RNA synthesis were further analyzed using the kinetic simulation program, PSUSIM, to obtain estimates of the intrinsic rate constants and the effect of T7 lysozyme on the rates of processes such as initiation, transition from initiation to elongation, and elongation. The KINSIM simulation program (Barshop et al., 1983) allows one to fit time courses of reaction to specific mechanisms and thus to determine the intrinsic kinetic rate constants. The process involves choosing a reasonable mechanism. The program calculates the differential equations for the mechanism and solves them by the method of numerical integration to yield simulated time courses (Frieden, 1994). The simulated kinetic curves are then compared to the experimental time courses, and the rate constants are adjusted to obtain the best fit between simulated and real data.

We have assumed the simplified mechanism shown in Scheme 1a to describe the transcription process. It is clear that the formation of RNA products during transcription occurs in two stages: 2−8-mer RNAs are synthesized in the first stage, and some intermediate but mostly runoff products are synthesized in the second stage. The synthesis of 2−8-mer (abortive RNA synthesis) is summed into one step (k_1), which is limited by the rate of transcription initiation. The synthesis of elongation products, 9−19-mer, is limited by the rate of transition from initiation to elongation (k_2). Both the abortive and elongation products dissociate from the enzyme at an average rate constant of k_3 and k_4,

Scheme 1

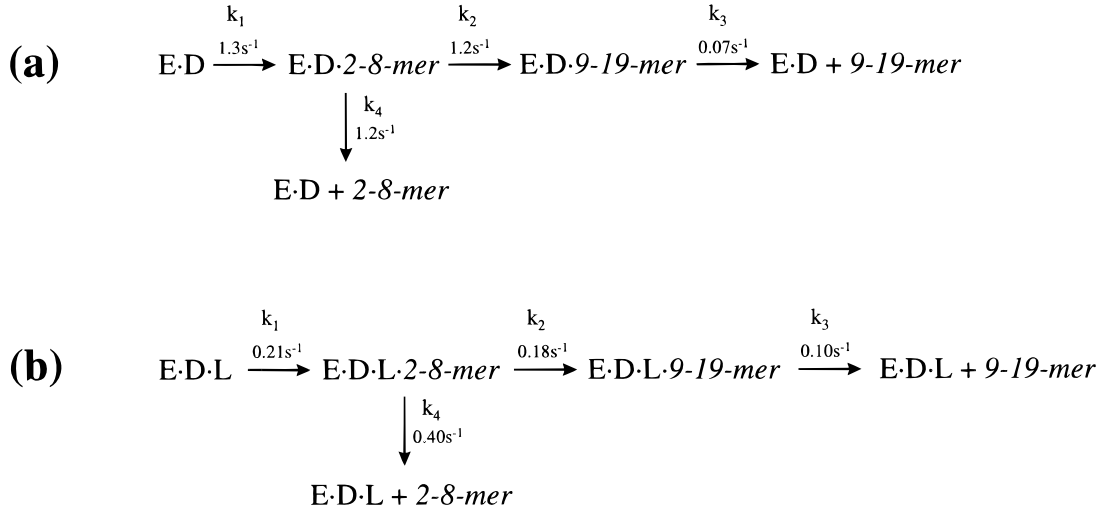

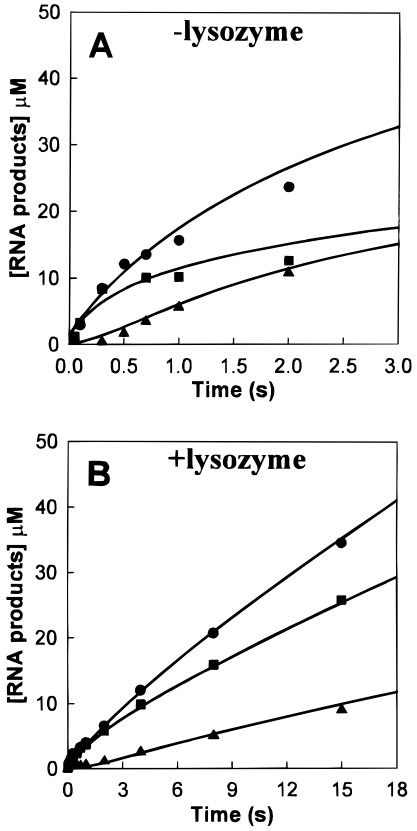

FIGURE 6: Kinetic simulation of transcription reaction in the absence and presence of T7 lysozyme. The pre-steady-state kinetic data shown in Figure 5 were simulated using the simulation program PSUSIM. Panels A and B show the pre-steady-state kinetics of RNA synthesis, 2−19-mer (●), 2−8-mer (■), and 9−19-mer (▲) in the absence and the presence of T7 lysozyme respectively. The solid lines are simulated curves predicted by the mechanism in Scheme 1a and 1b in the absence and presence of T7 lysozyme respectively.

respectively. The best global fit (Figure 6A) to the observed pre-steady-state kinetic data (from Figure 5) describing total, abortive, and elongation RNA product formation revealed that the 2−8-mer products were formed with a composite rate constant of 1.3 s^{-1} and that the 9−19-mer RNA products were formed with a composite rate constant of 1.2 s^{-1}. Since very little intermediate RNA products accumulated after 2−8-mer formation, the 9−19-mer RNA products are most likely limited by a slow step during the transition from initiation to elongation. The average rate constant of abortive RNA product dissociation was 1.2 s^{-1}, and the kinetics fit best to elongation products dissociating at an average rate of 0.07 s^{-1}. It was clear from the simulation process that the dissociation of abortive and runoff products largely dictated the steady-state rate of total RNA synthesis.

We then simulated the kinetics of transcription in the presence of T7 lysozyme using the mechanism shown in Scheme 1b. The best global fit (shown in Figure 6B) of the observed pre-steady-state kinetics in the presence of T7 lysozyme (data from Figure 5) provided the rate constants of the individual steps in the transcription reaction shown in Scheme 1b. Comparison of the derived rate constants in the absence and presence of T7 lysozyme (Scheme 1a and b) showed that the first step, that is initiation, was inhibited about 6-fold by T7 lysozyme, and the second step, the transition from initiation to elongation, was also inhibited by about the same extent. Dissociation of abortive products was inhibited about 3-fold (k_3) and T7 lysozyme had less of an effect on the dissociation of elongation or runoff products (k_4).

T7 Lysozyme Does Not Affect the Equilibrium Polymerase−Promoter DNA Interaction

One mechanism by which T7 lysozyme could inhibit transcription initiation is by weakening the interactions of the RNA polymerase for the promoter DNA. To investigate this possibility, we have measured the equilibrium and kinetic interactions between the polymerase and the 40 bp Φ10 promoter in the absence and presence of T7 lysozyme. The equilibrium binding of Φ10 promoter DNA to the RNA polymerase was investigated using the nitrocellulose DNA binding assay. The nitrocellulose DNA binding assay is not an ideal method for measuring the equilibrium K_d value, however it provided a qualitative answer as to whether T7 lysozyme prevented the polymerase from binding to the DNA. We could not use the previously reported fluorometric method (Jia et al., 1996) to quantitate the protein·DNA interactions because the high concentration of T7 lysozyme (10 μM) resulted in high background fluorescence. The nitrocellulose binding experiment was first carried out by titrating a constant amount of T7 RNA polymerase with increasing concentration of 5′ ^{32}P radiolabeled Φ10 DNA

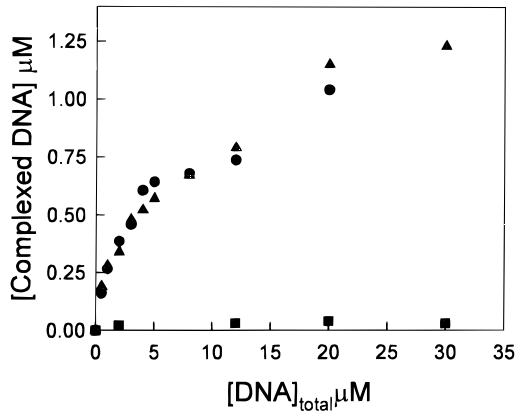

FIGURE 7: Equilibrium binding of T7 RNA polymerase to the promoter DNA in the presence and absence of T7 lysozyme. A constant amount of the polymerase (3 μM) was titrated with increasing amounts of 5′ ^{32}P labeled 40-mer Φ10 promoter DNA in the absence (●) and in the presence (▲) of T7 lysozyme (10 μM). These binding experiments were performed using nitrocellulose binding assay described in the Experimental Procedures. The titration of T7 lysozyme alone with increasing DNA (■) showed almost no DNA binding.

in the absence of T7 lysozyme. The experiment was then repeated in the presence of T7 lysozyme at a concentration of 10 μM, which is well above the measured K_d of E·L complex. The DNA binding isotherms in the absence and in the presence of lysozyme are shown in Figure 7. The results show that the binding of Φ10 promoter DNA to T7 RNA polymerase is unaffected by the presence of T7 lysozyme. An experiment carried out under similar conditions but in the absence of the polymerase showed that T7 lysozyme itself does not bind to the DNA.

T7 Lysozyme Does Not Affect the Kinetics of Polymerase−Promoter DNA Interaction

Although T7 lysozyme did not affect the equilibrium interactions of E·D, it could still have an effect on the kinetics of protein−DNA interactions. That is, it could slow down E·D complex formation which in turn could be responsible for the inhibition of overall transcription. Stopped-flow studies were carried out to determine the association and dissociation rate constants of Φ10 promoter−polymerase binary complex formation in the presence and absence of T7 lysozyme. As reported previously (Jia et al., 1996), binding of DNA to the RNA polymerase leads to a change in intrinsic protein fluorescence. To measure the stopped-flow kinetics in the presence of T7 lysozyme, an E·L complex formed by preincubating T7 RNA polymerase (0.4 μM) with T7 lysozyme (1 μM) was mixed rapidly with increasing concentration of Φ10 promoter DNA and the time course of the decrease in protein fluorescence was measured. The kinetics of decrease in fluorescence fit to a single exponential function, and the observed rate constants were plotted *versus* [DNA] to obtain the k_{on} and k_{off} rate constants for DNA binding, as described previously (Jia et al., 1996). Table 1 lists the measured k_{on}, k_{off}, and K_d values in the absence and presence of T7 lysozyme. The data showed that T7 lysozyme had only a marginal effect on the k_{on} and k_{off} rate constants of E binding to D, and on the K_d of the E·D complex. This is in agreement with the results of the nitrocellulose DNA binding experiments.

We wished to test if higher concentrations of T7 lysozyme would have an effect on the kinetics of polymerase binding to the promoter DNA. The presence of 10 μM concentration of T7 lysozyme resulted in increased background fluorescence which made measurement of small changes in protein fluorescence upon E·D complex formation very difficult. To overcome this problem, we have used 2-AP Φ10 DNA, where the dAs in the initiation region (−4 to +4) were replaced with a fluorescent analog, 2-aminopurine (2-AP) (Jia et. al., 1996). We then monitored the change in 2-AP DNA fluorescence upon binding to the polymerase. The results (Table 1) showed that even in the presence of a high concentration of lysozyme, the kinetics of RNA polymerase binding to DNA remained unaffected.

Table 1: Kinetic Constants of E·D Complex Formation in the Presence or Absence of T7 Lysozyme

promoter	k_{on} (μM^{-1} s^{-1})	k_{off} (s^{-1})	$k_{off}/k_{on} = K_d$ (μM)	[L] (final, μM)
Φ10	83	4.1	0.049	−
Φ10	67	3.0	0.045	0.5
2APΦ10	95	3.6	0.038	10.0

DISCUSSION

We have investigated here the mechanism of transcription repression by T7 lysozyme protein. Besides its function in cell lysis during phage infection, T7 lysozyme is a repressor of T7 RNA polymerase. It has been shown previously that T7 lysozyme forms a complex with T7 RNA polymerase, but the exact mechanism by which lysozyme inhibits transcription is not known. In this study, we have quantitated the interactions between the two proteins and have identified the macroscopic steps during transcription that are affected by T7 lysozyme. By measuring the kinetics of association and dissociation of E·L complex using stopped-flow kinetics, we have determined that T7 lysozyme forms a complex with the T7 RNA polymerase with a K_d of about 0.1 μM. T7 lysozyme binds to the RNA polymerase with almost diffusion-controlled rate constant, but the complex also dissociates with a fairly fast rate constant of 3.5 s^{-1}. This fast dissociation rate constant explains recent results of Zhang and Studier (1997) where labeled T7 lysozyme in the E·L complex was found to rapidly exchange with added unlabeled T7 lysozyme. They used native gel electrophoresis to analyze E·L complex formation and also showed that polymerase forms a 1:1 complex with T7 lysozyme.

Unlike most repressors that appear to inhibit transcription by acting as blocks to movement of polymerase on the DNA (Record et al., 1996), T7 lysozyme seems to have a different mechanism of inhibition. It does not form a stable complex with the promoter or a nonpromoter DNA, and it does not compete with the RNA polymerase for binding to the promoter DNA as indicated by our results and those of Zhang and Studier (1997). In addition, T7 lysozyme does not affect the kinetic or the thermodynamic interactions of the polymerase with the promoter DNA as our stopped-flow kinetics results show that the k_{on}, k_{off}, and K_d of E·D complex formation remained unchanged in the presence of T7 lysozyme. All the studies thus far are consistent with a model whereby RNA polymerase, the promoter DNA, and T7 lysozyme form a ternary complex, E·D·L, that has lower or inhibited transcription activity.

A combination of pre-steady-state and the steady-state kinetic studies allows measurement of the rates of initiation,

of transition from initiation to elongation, and of polymerase cycling or RNA dissociation (Jia & Patel, 1997). Such kinetic studies in the absence and presence of lysozyme at a 40-mer Φ10 promoter DNA showed that lysozyme inhibits both transcription initiation and formation of elongation or runoff products. Because the steady-state rate of RNA synthesis remained unchanged in the presence of T7 lysozyme, RNA product dissociation or polymerase cycling steps are not affected by T7 lysozyme. The step that limits transcription initiation at the Φ10 promoter is the formation of pppGpG, the first RNA product formed by phosphodiester bond formation between two GTPs. Since T7 lysozyme inhibits transcription initiation, it inhibits either the pppGpG formation step or a step prior to pppGpG synthesis. Although the present studies have not determined the exact step that is inhibited by T7 lysozyme, we have shown that DNA binding to the polymerase is not affected by T7 lysozyme. Thus, T7 lysozyme could inhibit steps such as open complex formation, GTP binding, or any conformational changes prior to pppGpG formation.

T7 lysozyme also affects the synthesis of elongation products or runoff product. The inhibition of the runoff product may be due to inhibition of the elongation process itself or due to inhibition of the transition from initiation to elongation. In the absence of lysozyme, the transition from initiation to processive elongation is a slow process; therefore, it is very likely that T7 lysozyme affects the transition step rather than elongation. This idea is consistent with the results of Zhang and Studier (1997), which showed that once the polymerase is in the elongation phase, it was not sensitive to inhibition by T7 lysozyme. The inhibition of runoff products appeared to be more dramatic than the inhibition of abortive products. This is due to the cumulative effect of T7 lysozyme inhibiting the initiation as well as the transition from initiation to elongation steps, both of which must occur before elongation. Thus, T7 lysozyme appears to inhibit mainly the early steps during transcription. It is not known whether T7 lysozyme cannot inhibit the polymerase in the elongation mode or if it cannot form a complex with the polymerase in the elongation mode. In the absence of T7 lysozyme, transcription initiation and transition from initiation to elongation are the slowest steps that limit RNA synthesis. It is interesting that T7 lysozyme affects both of these steps. This raises the question: Are these two processes, initiation and transition from initiation to elongation, limited by a common step which is then targeted by T7 lysozyme? Due to its simplicity, T7 RNA polymerase/T7 lysozyme is an ideal model system for the detailed quantitative studies which need to be carried out in order to understand the mechanism of repression. Future studies of T7 lysozyme inhibition will therefore provide interesting insights into mechanisms by which transcription can be regulated by protein−protein interactions.

REFERENCES

Barshop, B. A., Wrenn, R. F., & Frieden, C. (1983) *Anal. Biochem. 130*, 134−145.
Cheng, X., Zhang, X., Pflugrath, J. W., & Studier, F. W. (1994) *Proc. Natl. Acad. Sci. U.S.A. 91*, 4034−4038.
Davanloo, P., Rosenberg, A. H., Dunn, J. J., & Studier, F. W. (1984) *Proc. Natl. Acad. Sci. U.S.A. 81*, 2035−2039.
Frieden, C. (1994) *Methods Enzymol. 240*, 311−322.
Grodberg, J., & Dunn, J. J. (1988) *J. Bacteriol. 170*, 1245−1253.
Hingorani M. M., & Patel, S. S. (1993) *Biochemistry 32*, 12478−12487.
Jia, Y., & Patel, S. S. (1997) *Biochemistry 36*, 4223−4232.
Jia, Y., Kumar, A., & Patel, S. S. (1996) *J. Biol. Chem. 271*, 30451−30458.
Johnson, K. A. (1992) *The Enzymes* (Sigman, D. S., Ed.) 3rd ed., Vol. 20, pp 1−61.
King, G. C., Martin, C. T., Pham. T. T., & Coleman, J. E. (1986) *Biochemistry 25*, 36−40.
McAllister, W. T., & Wu, H.-L. (1978) *Proc. Natl. Acad. Sci. U.S.A. 75*, 804−808.
McAllister, W. T., Morris, C., Rosenberg, A. H., & Studier, F. W. (1981) *J. Mol. Biol. 153*, 527−544.
Moffatt, B. A., & Studier F. W. (1987) *Cell 49*, 221−227.
Record, M. T., Jr., Reznikoff, W. S., & Schlax, P. J. (1996) in *Escherichia coli and Salmonella typhimurium: Cellular and Molecular Biology*, 2nd ed., pp 792−820, American Society for Microbiology, Washington, DC.
Silberstein, S., Inouye, M., & Studier, F. W. (1975) *J. Mol. Biol.* 96, 1−11.
Sousa, R., Chung, Y. J., Rose, J. P., & Wang, B. C. (1993) *Nature 364*, 593−599.
Studier F. W. (1972) *Science 176*, 367−376.
Zhang, X., & Studier, F. W. (1995) *J. Mol. Biol. 250*, 156−168.
Zhang, X., & Studier, F. W. (1997) *J. Mol. Biol. 269*, 10−27.

BI971432Y